

Compact Dual-Frequency Fiber Laser Accelerometer With Sub- μg Resolution

Qian CAO, Long JIN^{*}, Yizhi LIANG, Linghao CHENG, and Bai-Ou GUAN

Guangdong Provincial Key Laboratory of Optical Fiber Sensing and Communications, Institute of Photonics Technology, Jinan University, Guangzhou, 510632, China

*Corresponding author: Long JIN E-mail: iptjinlong@gmail.com

Abstract: We demonstrate a compact and high-resolution dual-polarization fiber laser accelerometer. A spring-mass like scheme is constructed by fixing a 10-gram proof mass on the laser cavity to transduce applied vibration into beat-frequency change. The loading is located at the intensity maximum of intracavity light to maximize the optical response. The detection limit reaches $107 \text{ ng/Hz}^{1/2}$ at 200 Hz. The working bandwidth ranges from 60 Hz to 600 Hz.

Keywords: Dual-frequency fiber lasers; fiber Bragg grating; photonic accelerometers

Citation: Qian CAO, Long JIN, Yizhi LIANG, Linghao CHENG, and Bai-Ou GUAN, "Compact Dual-Frequency Fiber Laser Accelerometer With Sub- μg Resolution," *Photonic Sensors*, 2016, 6(2): 115–120.

1. Introduction

High-resolution accelerometer is an essential device in geophysical applications. Fiber-optic accelerometers have presented inherent advantages including high responsivity, low temperature cross sensitivity, and immunity to electromagnetic interference [1, 2]. To date, photonic accelerometers have been demonstrated in many different schemes to attain higher detection limit. Interferometric accelerometers have been fabricated by using a compliant cylinder or a central/edge-supported flexural disc to elongate optical fibers [3–5]. An accelerometer with a minimum detectable acceleration of $84 \text{ ng/Hz}^{1/2}$ has been achieved with 75-meter long optical fiber [4]. Fiber Bragg grating based accelerometers have attracted great interests due to the much shorter sensing element [6–8]. For example, the fiber Bragg grating (FBG) accelerometer based on a double-diaphragm

structure has exhibited a resolution of $385 \mu\text{g/Hz}^{1/2}$. Fiber laser accelerometers have higher detection capability as a result of the narrow linewidth of the laser output and the interrogation based on phase detection. For example, a fiber laser accelerometer with $126 \text{ ng/Hz}^{1/2}$ resolution has been achieved by directly stressing the laser with a proof mass [8].

Alternatively, single-longitudinal-mode fiber lasers with the orthogonal polarization output have been exploited as high resolution sensors, by monitoring the beat frequency in the radio frequency (RF) domain [9, 10]. In this paper, we demonstrate a high-resolution dual-polarization fiber laser accelerometer. The accelerometer is fabricated by simply fixing a 10-gram proof mass on the laser cavity at the light intensity maximum, to effectively transduce applied vibration to beat-frequency variation. The accelerometer presents a resolution of $107 \text{ ng/Hz}^{1/2}$ at 200 Hz and a working bandwidth from 60 Hz to 600 Hz. This accelerometer presents

Received: 14 January 2016 / Revised: 1 March 2016

© The Author(s) 2016. This article is published with open access at Springerlink.com

DOI: 10.1007/s13320-016-0315-y

Article type: Regular

sub- μg detection limit with a weight of only tens of grams, which is greatly beneficial for geophysical applications.

2. Dual-frequency fiber grating laser

Figure 1 shows the schematic of the sensing element, i.e., a fiber grating laser, fabricated by photoinscribing two wavelength-matched, highly reflective (typically higher than 25 dB) intracore Bragg gratings in an Er-doped fiber. Due to the imperfection in symmetry of the fiber core and the ultraviolet (UV) side illumination, the lasing frequencies ν_x and ν_y of the two orthogonal polarization modes are somewhat different, yielding a radio-frequency beat signal. The beat frequency is mainly determined by the intracavity birefringence by $\nu = |\nu_x - \nu_y| = cB/n_0\lambda$, where B denotes the birefringence, c is the vacuum light speed, and n_0 represents the average mode index.

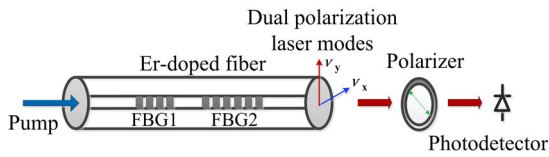


Fig. 1 Schematic of the dual-polarization fiber grating laser.

Figure 2 shows the measured spectrum of the beat signal of a fiber grating laser in an Er-doped fiber (M-12, Fiber Core Ltd.). The gratings are 5.5 mm and 4.5 mm in length and 31 dB and 29.6 dB in coupling strength, respectively. The grating separation is about 2 mm. We intend to reduce the separation as possible to approach the distributed feedback (DFB) structure. The lasing wavelength is 1553 nm, determined by the pitch of the phase mask. The beat signal is measured by use of a vector signal analyzer (MS2692A, Anritsu), which incorporates a frequency demodulator with extremely high frequency resolution, with 1 kHz resolution bandwidth. The beat frequency is 371.65 MHz, corresponding to a birefringence 2.78×10^{-6} of the fiber. The signal-to-noise ratio is higher than 60 dB. The laser can be exploited as a photonic sensor by

transducing the measurands into beat frequency variation.

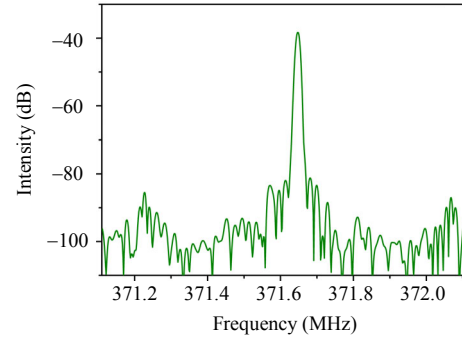


Fig. 2 Measured frequency spectrum of the output beat signal.

3. Sensitivity and noise

The accelerometer has a spring-mass configuration, which involves transversely loading the cavity with a proof mass. The frequency responsivity can be characterized by use of the mechanical susceptibility, expressed by [11]

$$\chi^{-1} = \omega_m^2 - \omega^2 + i \frac{\omega_m \omega}{Q_m} \quad (1)$$

where ω and ω_m represent the frequencies of applied vibration and the m th order natural frequency, and Q_m is the quality factor of the resonator. This expression indicates that the responses at the frequency range below the fundamental resonance frequency are very close to the static response. Here, we can alternatively analyze the optical response of the laser sensor to a static load. Since the beat frequency is originated from the round-trip phase difference between the two polarization modes, the response in terms of beat-frequency shift to a localized perturbation is highly dependent on the local intensity, which can be expressed by

$$\Delta\nu = \frac{c}{n_0\lambda} \int_{-\infty}^{+\infty} \Delta B(z) I(z) dz \quad (2)$$

where ΔB is the induced local birefringence which is in proportion to the applied load, and I represents the local intensity normalized by $\int_{-\infty}^{+\infty} I(z) dz = 1$. The intensity profile of an ideal DFB laser can be

expressed by

$$I(z) = \kappa \cdot e^{-2\kappa|z|} \quad (3)$$

where κ (m^{-1}) represents the grating coupling coefficient. The intensity profile presents a peak at the phase shift point where $z=0$, yielding a maximum sensitivity at this point. Equation (3) indicates that the sensitivity is proportional to the grating coupling strength.

Figure 3 shows the measured longitudinal sensitivity profile by scanning the loading position with a glass rod of 5.1 gram rolling along the fiber length via quasi-point contact by use of the setup described in [12]. The fiber laser is placed on an inclined plane with the angle $\theta=17^\circ$ between the horizontal and inclined planes. Meanwhile, an ordinary singlemode fiber is placed parallel to the fiber laser as a support fiber to keep the balance of the rod. Therefore, the normal force subjected to the laser is $N=mg\cos\theta/2=2.39\times 10^{-2}$ N. In this measurement as well as the accelerometer implementation in the following text, the load is applied in accordance with principle axis of the fiber to maximize the sensitivity. The measured curve presents a single peak in between the two gratings, in accordance with the measured intensity profile in [13]. The maximum sensitivity can be calculated as 72 MHz/gram. Considering the grating coupling coefficient can be as high as 1000 m^{-1} in our experiment, the laser is expected to have a sensitivity as high as 100 MHz/gram. However, due

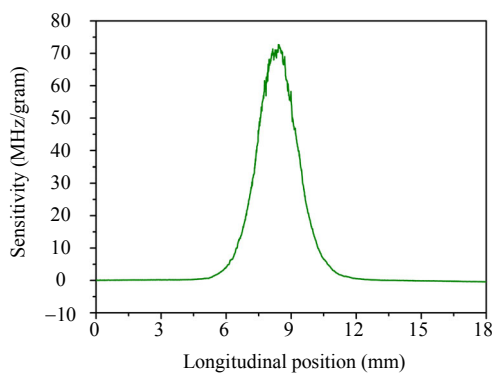


Fig. 3 Measured sensitivities of the fiber grating laser to a static transverse load along the fiber length.

to the limitation in fiber gain, we have to leave a certain separation between the two gratings to achieve laser oscillation. This deviation can be equivalently treated as a DFB laser with lower grating coupling strength or longer cavity length.

The frequency noise of a fiber grating laser with the single polarization mode output has been investigated in [14–16], and the dominate noise source is the nonequilibrium thermal fluctuation over the gain medium, yielding a $1/f$ profile over the low and intermediate frequencies (which are exactly the frequency ranges of interest). The two polarization modes of the present laser share the same cavity and have a high correlation degree. As a result, the noise level of the beat signal also presents the $1/f$ profile but is much lower than each polarization mode [15]. The noise spectral density can be simply expressed by $S(f)=C/f$, where C represents the noise strength. Figure 4 shows the measured spectral density profile of the frequency noise. The C value is estimated as $C=2.2\times 10^5$ (Hz^2) via exponential fit. Generally speaking, active fibers with higher concentration can produce a higher noise level. Note that the noise level is also related to the intensity profile. It can be approximately considered proportional to the item $\sqrt{\int I^2(z)dz}$. Substituting the intensity profile depicted by (3), the noise level of a dual-polarization laser is proportional to $\sqrt{\kappa}$. This fiber is selected for accelerometer fabrication because it produces relatively low noise level among the individual

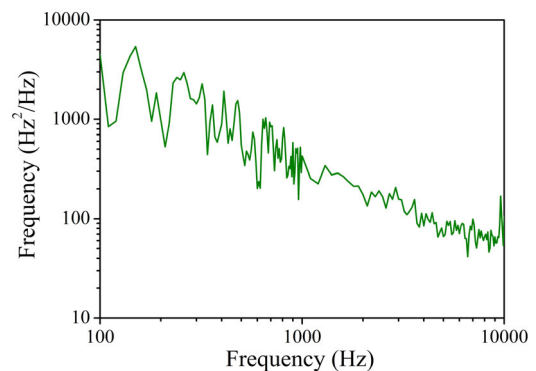


Fig. 4 Measured frequency noise of the beat signal.

products and can provide sufficient photosensitivity for grating inscription. In addition, the noise level is irrelevant with the power and the wavelength of the pump laser.

Regardless of the frequency demodulation capability, the detection capability of the laser sensor can be characterized by the ratio of sensitivity over noise, which is proportional to $\sqrt{\kappa}$. That means the higher grating coupling strength (or shorter effective cavity length) can result in lower detection limit. That is why we intend to shorten the laser cavity in the implementation of the laser accelerometer.

4. Implementation and characterization of the accelerometer

Figure 5 shows the experimental setup of the fiber laser accelerometer. A 10-gram proof mass is fixed onto the laser cavity at the intensity maximum. The contact length between the mass and the laser cavity is about 2 mm. In this mass-spring like structure, the fiber laser acts as a “spring”. When the sensor package is subjected to vertical vibration, the proof mass periodically squeezes the fiber and consequently causes a beat-frequency shift. The amplitude, frequency, and phase of the applied vibration can be optically interrogated by reading out the beat frequency shift. A dummy fiber is placed parallel to the lasing fiber to keep balance of the structure. The fiber grating laser is pumped with a 980 nm laser diode via a wavelength division multiplexer (WDM). An in-line polarizer is used to maximize the intensity of the beat signal. A reference sensor is also attached on the exciter for calibration. Compared with our previous work based on the cantilever based transducer [17], the present structure has higher transducing efficiency. This configuration can be highly compact, compared to transducers for the single-frequency fiber laser accelerometers like the ones described in [8].

Figure 6 shows the measured beat-frequency deviation as a function of acceleration amplitude at

480 Hz. The accelerometer demonstrates a linear response versus vibration strength. Figure 6 inset shows a typical sensor output in terms of beat-frequency variation measured by the signal analyzer. The applied acceleration is 6.34 mg.

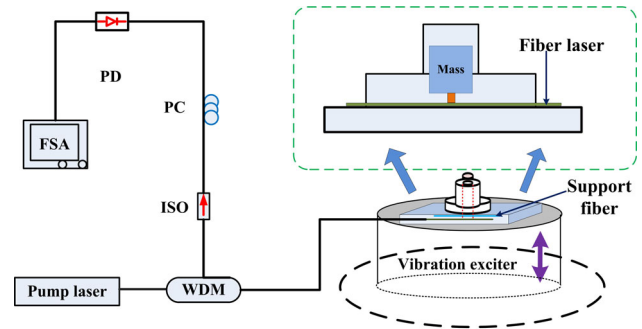


Fig. 5 Experimental setup of the fiber laser accelerometer (WDM: wavelength division multiplexer; ISO: isolator; PC: polarization controller; PD: photodetector; VSA: vector signal analyzer).

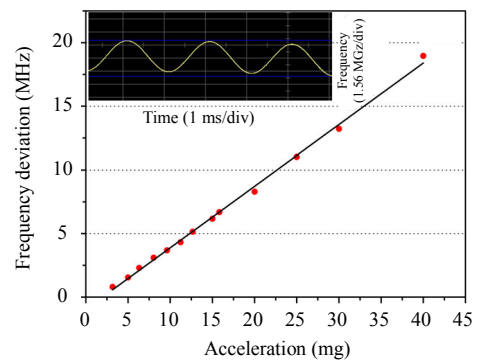


Fig. 6 Measured frequency deviation as a function of acceleration amplitude at 480 Hz (inset: typical output signal under variation with a frequency of 480 Hz and an amplitude of 6.34 mg).

Figure 7 shows the average sensitivity below 600 Hz is estimated as 290 MHz/g ($1g = 9.8 \text{ m/s}^2$). The fundamental natural frequency is about 680 Hz as a result of resonance effect. The sensor presents a broad and flat frequency range from 60 Hz to 600 Hz as the operating bandwidth. This natural frequency is much lower than our calculated result, due to the out-of-phase vibration arising from the imperfection of the transducer fabrication. The minimal detectable signal is fundamentally limited by the frequency noise of the beat signal in Fig. 4. For example, the frequency noise at 200 Hz is about

971 Hz^2/Hz (31.2 $\text{Hz}/\text{Hz}^{1/2}$). Considering the sensitivity of 290 MHz/g and the sensitivity-to-noise ratio (SNR) of 139.3 $\text{dB}/\text{g}/\text{Hz}^{1/2}$, the minimal detectable acceleration is estimated as about 107 $\text{ng}/\text{Hz}^{1/2}$ at 200 Hz .

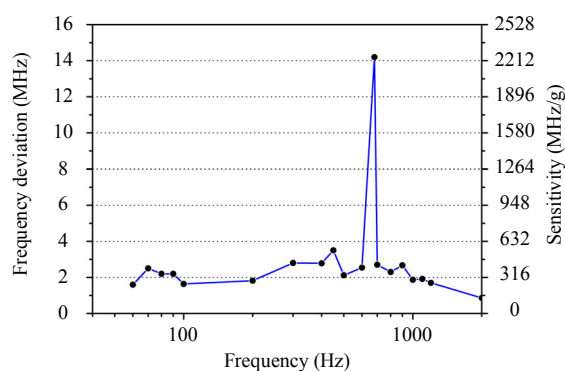


Fig. 7 Measured frequency response and related sensitivities with an acceleration amplitude of 6.34 mg .

5. Conclusions

In summary, we have demonstrated a high-resolution accelerometer based on a dual-polarization fiber grating laser with a device weight only tens of grams. A resolution of 107 $\text{ng}/\text{Hz}^{1/2}$ at 200 Hz has been attained with a spring-mass like transducer scheme. Theoretical and experimental investigations reveal that an ideal DFB fiber laser with higher grating coupling strengths (or shorter effective cavity length) can enable higher detection capability to the applied load. The further performance improvement relies on both the fabrication of an active fiber with both high UV photosensitivity and optical gain and the improvement of the transducer fabrication.

Acknowledgment

This work is supported by the National Natural Science Foundation of China (Nos. 61235005 and 11474133), Guangdong Natural Science Foundation (No. S2013030013302), and the Planned Science & Technology Project of Guangzhou (Nos. 2012J510028 and 2014J2200003). L. Jin is supported by the Department of Education, Guangdong Province (No. Yq2013021) and by Open

Fund of the Guangdong Provincial Key Laboratory of Fiber Laser Materials and Applied Techniques (South China University of Technology).

Open Access This article is distributed under the terms of the Creative Commons Attribution 4.0 International License (<http://creativecommons.org/licenses/by/4.0/>), which permits unrestricted use, distribution, and reproduction in any medium, provided you give appropriate credit to the original author(s) and the source, provide a link to the Creative Commons license, and indicate if changes were made.

References

- [1] X. Wu, X. Wang, S. Li, S. Huang, Q. Ge, and B. Yu, "Cantilever fiber-optic accelerometer based on modal interferometer," *Photonics Technology Letters*, 2015, 27(15): 1632–1635.
- [2] Y. Liu, W. Peng, X. Zhang, Y. Liang, Z. Gong, and M. Han, "Fiber-optic anemometer based on distributed Bragg reflector fiber laser technology," *Photonics Technology Letters*, 2013, 25(13): 1246–1249.
- [3] N. Zeng, C. Z. Shi, M. Zhang, L. W. Wang, Y. B. Liao, and S. R. Lai, "A 3-component fiber-optic accelerometer for well logging," *Optics Communications*, 2004, 234(1–6): 153–162.
- [4] G. A. Cranch and P. J. Nash, "High-responsivity fiber-optic flexural disk accelerometers," *Journal of Lightwave Technology*, 2000, 18(9): 1233–1243.
- [5] G. Chen, X. Zhang, G. Brambilla, and T. P. Newson, "Theoretical and experimental demonstrations of a microfiber-based flexural disc accelerometer," *Optics Letters*, 2011, 36(18): 3669–3671.
- [6] Q. Liu, X. Qiao, Z. Jia, H. Fu, H. Gao, and D. Yu, "Large frequency range and high sensitivity fiber Bragg grating accelerometer based on double diaphragms," *IEEE Sensors Journal*, 2014, 14(5): 1499–1504.
- [7] Q. Liu, X. Qiao, J. Zhao, A. Zhen, H. Gao, and M. Shao, "Novel fiber Bragg grating accelerometer based on diaphragm," *IEEE Sensors Journal*, 2012, 12(12): 3000–3004.
- [8] G. H. Ames and J. M. Maguire, "Erbium fiber laser accelerometer," *IEEE Sensors Journal*, 2007, 7(4): 557–561.
- [9] B. Guan, L. Jin, Y. Zhang, and H. Tam, "Polarimetric heterodyning fiber grating laser sensors," *Journal of Lightwave Technology*, 2012, 30(8): 1097–1111.
- [10] K. Yu, C. Lai, C. Wu, Y. Zhao, C. Lu, and H. Tam, "A high-frequency accelerometer based on distributed Bragg reflector fiber laser," *Photonics Technology Letters*, 2014, 26(14): 1418–1421.

- [11] A. G. Krause, M. Winger, T. D. Blasius, Q. Lin, and O. Painter, "A microchip optomechanical accelerometer," *Nature Photonics*, 2012, 6(11): 768–772.
- [12] F. Zhou, L. Jin, Y. Liang, L. Cheng, and B. Guan, "Spatial sensitivity characterization of dual-polarization fiber grating laser sensors," *Journal of Lightwave Technology*, 2015, 33(19): 4151–4155.
- [13] S. Foster and A. Tikhomirov, "Experimental and theoretical characterization of the mode profile of single-mode DFB fiber lasers," *Quantum Electronics*, 2005, 41(6): 762–766.
- [14] O. Llopis, P. H. Merrer, H. Brahim, K. Saleh, and P. Lacroix, "Phase noise measurement of a narrow linewidth CW laser using delay line approaches," *Optics Letters*, 2011, 36(14): 2713–2715.
- [15] S. Foster, G. A. Cranch, and A. Tikhomirov, "Experimental evidence for the thermal origin of $1/f$ frequency noise in erbium-doped fiber lasers," *Physical Review A*, 2009, 79(5): 1744–1747.
- [16] S. Foster, "Fundamental limits on $1/f$ frequency noise in rare-earth-metal-doped fiber lasers due to spontaneous emission," *Physical Review A*, 2008, 78(1): 013820.
- [17] B. Guan, X. Sun, and Y. Tan, "Dual polarization fiber grating laser accelerometer," in *Proc. SPIE*, vol. 7653, pp. 76530Z-1–76530Z-4, 2010.